

# Galaxy And Mass Assembly (GAMA): the connection between metals, specific SFR and H I gas in galaxies: the Z–SSFR relation

M. A. Lara-López,<sup>1\*</sup>† A. M. Hopkins,<sup>1</sup> A. R. López-Sánchez,<sup>1,2</sup> S. Brough,<sup>1</sup>  
M. Colless,<sup>1</sup> J. Bland-Hawthorn,<sup>3</sup> S. Driver,<sup>4,5</sup> C. Foster,<sup>6</sup> J. Liske,<sup>7</sup> J. Loveday,<sup>8</sup>  
A. S. G. Robotham,<sup>4,5</sup> R. G. Sharp,<sup>9</sup> O. Steele<sup>10</sup> and E. N. Taylor<sup>3,11</sup>

<sup>1</sup>Australian Astronomical Observatory, PO Box 915, North Ryde, NSW 1670, Australia

<sup>2</sup>Department of Physics and Astronomy, Macquarie University, Sydney, NSW 2109, Australia

<sup>3</sup>Sydney Institute for Astronomy (SIfA), School of Physics, University of Sydney, Sydney, NSW 2006, Australia

<sup>4</sup>International Centre for Radio Astronomy Research, The University of Western Australia, 35 Stirling Highway, Crawley, WA 6009, Australia

<sup>5</sup>School of Physics & Astronomy, University of St Andrews, North Haugh, St Andrews KY16 9SS, UK

<sup>6</sup>European Southern Observatory, Alonso de Cordova 3107, Vitacura, Santiago, Chile

<sup>7</sup>European Southern Observatory, Karl-Schwarzschild-Str. 2, D-85748 Garching, Germany

<sup>8</sup>Astronomy Centre, University of Sussex, Falmer, Brighton BN1 9QH, UK

<sup>9</sup>Research School of Astronomy & Astrophysics, Australian National University, Cotter Road, Weston Creek, ACT 2611, Australia

<sup>10</sup>Institute of Cosmology and Gravitation, University of Portsmouth, Dennis Sciama Building, Burnaby Road, Portsmouth PO1 3FX, UK

<sup>11</sup>School of Physics, The University of Melbourne, Parkville, VIC 3010, Australia

Accepted 2013 April 14. Received 2013 March 7; in original form 2012 November 5

## ABSTRACT

We study the interplay between gas phase metallicity ( $Z$ ), specific star formation rate (SSFR) and neutral hydrogen gas ( $H\text{I}$ ) for galaxies of different stellar masses. Our study uses spectroscopic data from Galaxy and Mass Assembly and Sloan Digital Sky Survey (SDSS) star-forming galaxies, as well as  $H\text{I}$  detection from the Arecibo Legacy Fast Arecibo  $L$ -band Feed Array (ALFALFA) and Galex Arecibo SDSS Survey (GASS) public catalogues. We present a model based on the  $Z$ –SSFR relation that shows that at a given stellar mass, depending on the amount of gas, galaxies will follow opposite behaviours. Low-mass galaxies with a large amount of gas will show high SSFR and low metallicities, while low-mass galaxies with small amounts of gas will show lower SSFR and high metallicities. In contrast, massive galaxies with a large amount of gas will show moderate SSFR and high metallicities, while massive galaxies with small amounts of gas will show low SSFR and low metallicities. Using ALFALFA and GASS counterparts, we find that the amount of gas is related to those drastic differences in  $Z$  and SSFR for galaxies of a similar stellar mass.

**Key words:** galaxies: abundances – galaxies: fundamental parameters – galaxies: star formation – galaxies: statistics.

## 1 INTRODUCTION

The formation of galaxies is intimately dependent on the conversion of stars into gas, the production of heavy elements, recycling of this material into the interstellar medium (ISM) and repetitions of this cycle. A detailed understanding of the interplay between each of gas mass, star formation rate (SFR) and metallicity is clearly important to understand the galaxy evolution process. Scaling relations between SFR and stellar or gas mass, and between mass and

metallicity, have been explored for many years. More recently, the connection between gas fraction and metallicity has also begun to be explored (Hughes et al. 2013). Identifying the causal relationships between these empirical scaling relations is, however, more challenging.

From the fundamental properties of galaxies, we can identify extensive (scale-dependent) and intensive (scale-invariant) properties. Intensive properties are essential or inherent to a system and are independent of the amount of baryonic mass, for example metallicity, temperature, density and specific star formation rate (SSFR). Extensive properties, on the other hand, depend on the amount of baryonic mass of the system, such as the SFR and stellar mass ( $M_*$ ). By way of illustration of this point, if we were to split a galaxy in half,

\* E-mail: mlopez@ao.gov.au

† ARC Super Science Fellow

the metallicity of the halves is unchanged from the original galaxy. The SFR and stellar mass of the halves, however, are half that of the original, corresponding to the amount of baryonic mass removed.

Although the metallicity is scale invariant or intensive, it is related to the stellar mass through the well known  $M_*$ - $Z$  relation (e.g. Tremonti et al. 2004; Lara-López et al. 2009a,b). In this relationship, the metallicity of high-mass systems is higher than that of low-mass systems. This does not mean that the metallicity and  $M_*$  are dependent variables. A correlation or trend between an intensive and an extensive property cannot be directly causal. For example, simply combining a large number of low-metallicity dwarf galaxies will increase the total mass, but will not directly increase the metallicity of the total system. Any such relation, consequently, must imply a common underlying cause, in this example likely to be the star formation (SF) history of the galaxy.

On the other hand, relationships such as  $Z$ -SFR and  $Z$ -SSFR are shown to have weaker correlations (e.g. Lara-López et al. 2010; López-Sánchez 2010; Yates, Kauffmann & Guo 2012; Lara-López, López-Sánchez & Hopkins 2013a). Specifically, the  $Z$ -SSFR relation is formed by intensive properties of galaxies, and has not been widely studied since it shows high scatter. Nevertheless, metallicity is important for the ability of gas clouds to form stars, since it enables most of the gas cooling that will facilitate the SF (Leboucheiller et al. 2013).

Crucial information regarding galaxy properties is given by their neutral gas content. Large H I surveys such as the Arecibo Legacy Fast Arecibo  $L$ -band Feed Array (ALFALFA; Haynes et al. 2011) and the Galex Arecibo Sloan Digital Sky Survey (SDSS) Survey (GASS; Catinella et al. 2010), have provided new scaling relationships and dependences for the cool gas in galaxies.

The link between the gas metallicity and H I content in galaxies was studied in Zhang et al. (2009). Specifically, they study the H I dependence on the  $M_*$ - $Z$  relation using SDSS galaxies. They estimate empirically the H I content for  $10^5$  emission-line galaxies in the SDSS-data release (DR) 4, and find that gas-poor galaxies are more metal rich at fixed stellar mass. Hughes et al. (2013) confirm this result, from an investigation of the role of cold gas and environment on the  $M_*$ - $Z$  relation for 260 nearby late-type galaxies. They find that, at fixed stellar mass, galaxies with lower gas fractions typically also possess higher metallicities. In general, they observe that gas-poor galaxies are typically more metal rich, and demonstrate that the removal of gas from the outskirts of spirals increases the observed average metallicity by  $\sim 0.1$  dex.

Although some scaling relations with H I content have been studied, the interplay between metallicity and SSFR has not yet been analysed as a function of the gas content or stellar mass. The  $Z$ -SSFR relation is formed by intensive properties, and is a key relationship to study the different properties of high- and low-mass galaxies.

The gas mass is a direct measure of the available fuel in galaxies to form stars. The relation of this gas with metallicity, stellar mass and SSFR can tell us how fast a galaxy assembled stars in the past, the amount of stars it formed and how actively it is forming stars at present. The main goal of this paper is to analyse the interplay between all these properties to produce a general picture of the gas recycling process.

This paper is organized as follows. In Section 2 we detail the data used for this study, and in Section 3 we analyse the  $Z$ -SSFR relation and present a cartoon model based on it. In Section 4 we study scaling relations using H I data. Finally, in Section 5 we present our discussion and conclusions. Throughout we assume  $H_0 = 70 \text{ km s}^{-1} \text{ mpc}^{-1}$ ,  $\Omega_M = 0.3$  and  $\Omega_\Lambda = 0.7$ .

## 2 SAMPLE SELECTION

### 2.1 Optical data

We consider data for emission-line galaxies from two large surveys, the Galaxy and Mass Assembly (GAMA phase-I survey; Driver et al. 2011) and the SDSS-DR7 (Abazajian et al. 2009).

Data from the SDSS were taken with the 2.5 m telescope located at Apache Point Observatory (Gunn et al. 2006). We use the emission-line analysis of SDSS-DR7 galaxy spectra performed by the MPA-JHU data base<sup>1</sup>. From the full data set, we only consider objects classified as galaxies in the ‘main galaxy sample’ (Strauss et al. 2002) with apparent Petrosian  $r$  magnitudes in the range  $14.5 < m_r < 17.77$  and  $z < 0.33$ . We use gas metallicities measured as described in Tremonti et al. (2004), SFR estimates described in Brinchmann et al. (2004) and total stellar masses estimated as in Kauffmann et al. (2003a).

The GAMA phase-I is a spectroscopic survey with the 3.9 m Anglo-Australian Telescope using the 2dF fibre feed and AAOmega multi-object spectrograph. For full details of the survey selection and properties see Driver et al. (2011). SFRs measurements are based on the H $\alpha$  emission line as described in Gunawardhana et al. (2011). Metallicities were estimated using the empirical calibration provided by Pettini & Pagel (2004) between the oxygen abundance and the  $O3N2$  ( $([O \text{ III}] \lambda 5007/H\beta)/([N \text{ II}] \lambda 6583/H\alpha)$ ) index. Both SFRs and metallicities were recalibrated to the Bayesian system described above using the calibrations of Lara-López et al. (2013b). Finally, stellar masses were measured as described in Taylor et al. (2011).

For both surveys, we selected only SF galaxies using the standard spectroscopic diagnostic (Baldwin, Phillips & Terlevich 1981), and using the discrimination of Kauffmann et al. (2003b). For reliable metallicity and SFR estimates, we selected galaxies with a signal-to-noise ratio of 3 in H $\alpha$ , H $\beta$  and [N II]. Galaxies were selected in volume-limited samples in redshift and Petrosian  $r$ -band absolute magnitude as described in Lara-López et al. (2013b). Our final SF optical sample is 35 212 galaxies for GAMA and 156 910 for SDSS. These samples are used to match with ALFALFA and GASS data as described in the next section.

### 2.2 H I data

To test the correlations between optically derived properties and the H I content of galaxies, we used the ALFALFA (Haynes et al. 2011) and the GASS (Catinella et al. 2010) surveys.

ALFALFA is a blind survey of 21 cm H I emission over  $\sim 2800 \text{ deg}^2$  of sky. The public catalogue<sup>2</sup> provides  $\sim 15\,855$  H I detections, of which  $\sim 15\,041$  are associated with extragalactic objects. Since ALFALFA is a blind survey, we select only galaxies with Code = 1, which refers to robust, reliably detected sources. We also remove sources with heliocentric velocities  $V_{\text{helio}} < 100.0$ , which are unlikely to be galaxies. From this subsample, we cross-match RA, Dec. and redshift for our optical SF sample described in Section 2.1, obtaining a final sample of 4443 SF galaxies with ALFALFA counterparts. These come entirely from the SDSS, since the GAMA survey regions are not well covered by the publicly available ALFALFA data. Together with the fainter magnitude range of

<sup>1</sup> <http://www.mpa-garching.mpg.de/SDSS/>

<sup>2</sup> <http://egg.astro.cornell.edu/alfalfa/data/index.php>

the GAMA targets, this biases against them being identified with ALFALFA detections.

In order to increase our H I coverage of massive galaxies, we match our SDSS SF sample described in Section 2.1 with the GASS public catalogue. The GASS survey aims to observe a sample of  $\sim 1000$  galaxies selected from the SDSS spectroscopic and GALEX imaging surveys. GASS galaxies are selected to have stellar masses greater than  $10^{10} M_{\star}$  and redshifts  $0.025 < z < 0.05$ . The public catalogue includes 232 galaxies, from which we find 48 counterparts with our optical SF sample described in Section 2.1. The rest of the GASS galaxies correspond to composite and active galactic nuclei galaxies. The stellar mass range of our final sample is  $10^7 < M_{\star} < 10^{11} M_{\odot}$ , with a median of  $\sim 10^{9.3} M_{\odot}$ .

### 3 THE Z-SSFR RELATION

The correlation between the amount of metals and the SSFR has not been explored in detail. Since both Z and SSFR are intensive properties, this relationship provides a direct way to analyse the different properties of low- and high-mass galaxies.

Here, we explore the median SSFR in bins of Z for different  $M_{\star}$ . In Fig. 1, we show the Z-SSFR relation for SDSS and GAMA data. Each of the panels correspond to different redshifts of volume-limited samples as described in Lara-López et al. (2013b). The coloured circles correspond to the median SSFR in bins of Z for

different  $M_{\star}$ . Opposing trends are clearly observed in Figs 1(a) and (b) between low- and high-mass galaxies with an inflection point at  $\log(\text{SSFR}) \sim -9.9 \text{ yr}^{-1}$ . The SSFR for low-mass galaxies shows an anticorrelation with Z while the SSFR for high-mass galaxies correlates with Z.

#### 3.1 A model

We suggest that the opposite behaviours for low- and high-mass galaxies observed in Fig. 1 can be understood assuming that galaxies at a given  $M_{\star}$  have different amounts of H I. Based on that figure, we generate the cartoon model shown in Fig. 2. In this model, low-mass galaxies are represented by a blue ellipse that extends from high SSFR and low Z, to low SSFR and high Z. Massive galaxies, represented by a red ellipse, extend from low SSFR and low Z to high SSFR and high Z.

Different physical explanations can be given to justify this basic supposition of our cartoon model. The presence of galactic inflows and outflows and how they affect the metal enrichment in galaxies is still a matter of debate. Galactic outflows have been shown to be important to reproduce the  $M_{\star}$ -Z relation of galaxies using analytical (e.g., Erb 2008) and hydrodynamic models (e.g., Finlator & Davé 2008). On the other hand, Calura et al. (2009) reproduced the  $M_{\star}$ -Z relation mainly by means of an increasing efficiency of SF, without any need to invoke galactic outflows.

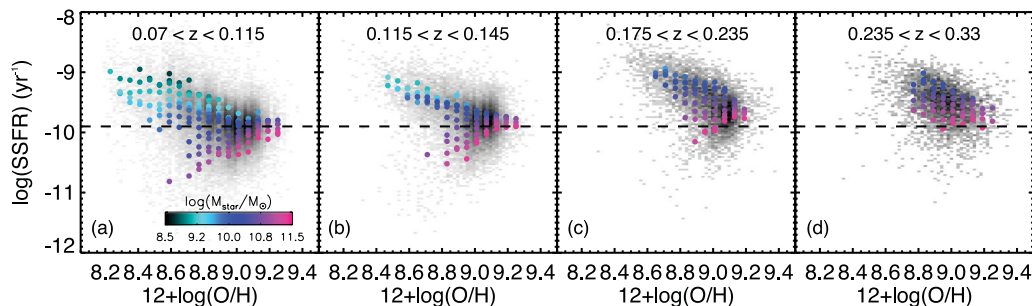


**Figure 1.** Z-SSFR relation for SDSS and GAMA data. The colour coded circles correspond to the median SSFR in bins of Z for different bins of  $M_{\star}$ . The grey points correspond to the density of SDSS and GAMA samples.

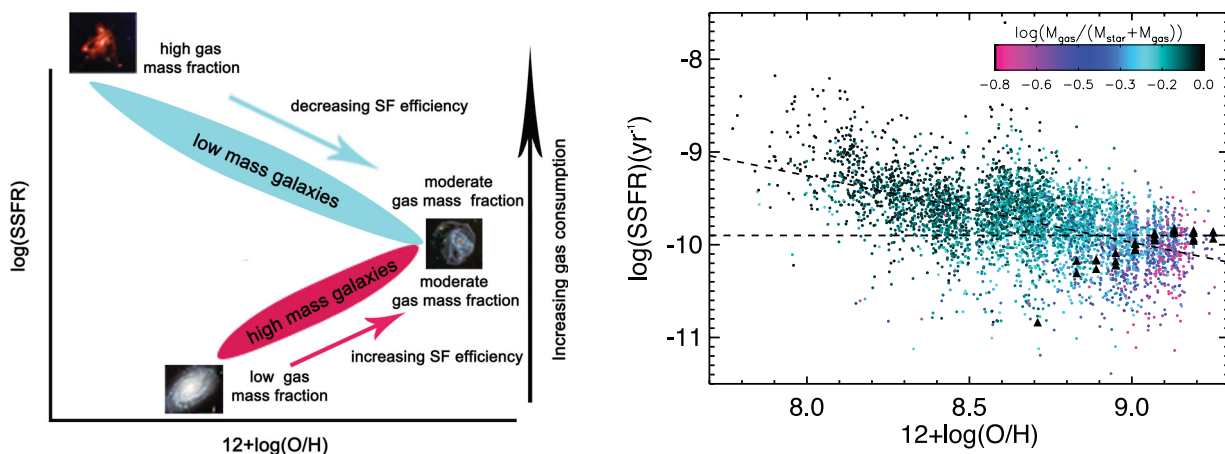


**Figure 2.** Left: cartoon model of the Z-SSFR relationship based on the extreme stellar mass cases of Fig. 1. The model is based on local redshift galaxies, and represents a snapshot of the behaviour of galaxies today. The blue and red ellipses represent low- and high-mass galaxies, respectively. Right: Z-SSFR relation for galaxies with ALFALFA and GASS counterparts. Galaxies are colour coded from low (magenta) to high (green) gas mass fraction. The black triangles show the median data for SDSS galaxies with no H I detection in the ALFALFA and GASS fields for  $\log(M_{\star}) > 11.0$  dex.

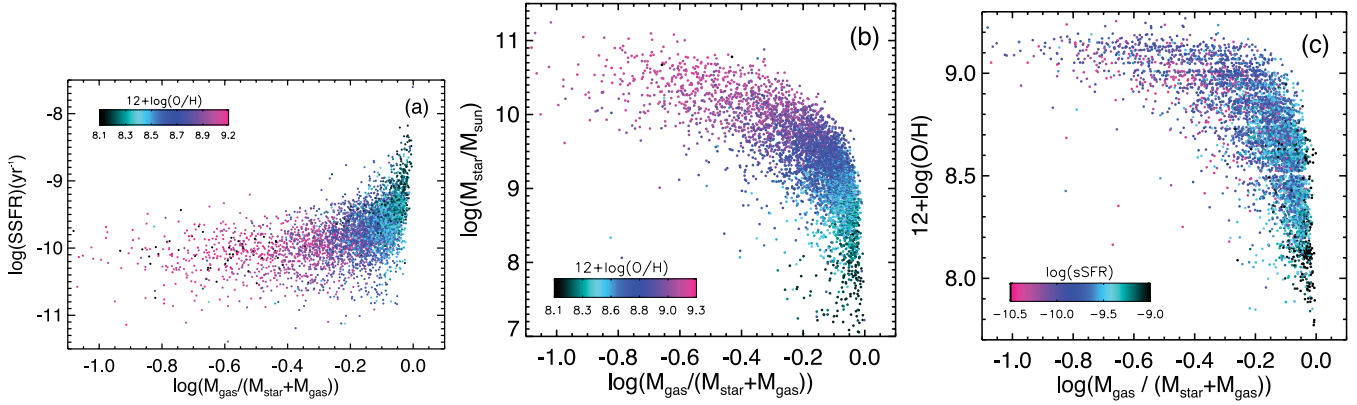


**Figure 3.** Scaling relations for SDSS galaxies with ALFALFA and GASS counterparts. (a) The gas mass fraction and SSFR relation colour coded from low (green) to high (magenta) metallicity. (b) The gas mass fraction and  $M_*$  relation colour coded as in (a). (c) The gas mass fraction and  $Z$  relation for the same sample colour coded from low (magenta) to high (green) SSFR.

A general picture of downsizing suggests that low-mass galaxies process their gas slower than massive galaxies, therefore, low-mass galaxies are actively forming stars, and present high SSFRs today compared to massive galaxies. Hereafter, we will focus on downsizing to provide a possible explanation for the trends between the intensive properties of SSFR and  $Z$  as a function of the extensive property of mass.

A combination of downsizing and the amount of  $H\text{I}$  can explain the opposing trends for low- and high-mass galaxies observed in the  $Z$ –SSFR relation. Focusing our attention on the low-mass galaxy branch (blue ellipse of Fig. 2), we can explain the differences in SSFR through the amount of  $H\text{I}$  present in each galaxy. Low-mass galaxies with a high amount of neutral gas will show higher SSFR today, as they have more fuel for SF, than galaxies of the same mass with a lower amount of neutral gas. The same is applicable to high-mass galaxies (red ellipse of Fig. 2), in this branch, galaxies with a high amount of  $H\text{I}$  show higher SSFRs than galaxies at the same mass with lower amount of  $H\text{I}$ .

It is noteworthy, however, that  $Z$  plays the opposite role. While low-mass galaxies with a large amount of  $H\text{I}$  show low  $Z$ , massive galaxies with a large amount of  $H\text{I}$  show high  $Z$ . This can again be explained by downsizing, but not downsizing in stellar mass, rather the amount of  $H\text{I}$  is driving the rate of metal enrichment in galaxies. In the low-mass branch, galaxies with large  $H\text{I}$  show low  $Z$  because they are processing their gas slower and on longer time-scales than galaxies with lower  $H\text{I}$  for the same stellar mass. On the other hand, massive galaxies with large  $H\text{I}$  show higher metallicities because they processed their gas faster in the past and have already reached high  $Z$ , and due to their large  $H\text{I}$ , they also have a high SSFR too.

#### 4 $H\text{I}$ SCALING RELATIONS

To test our model, we use the 4491 SDSS optical counterparts with direct  $H\text{I}$  mass measurements from the ALFALFA and GASS surveys described in Section 2.2. For the relationships shown in this section, we define the gas mass as  $M_{\text{gas}} = 1.32 \times M_{H\text{I}}$ , and the gas mass fraction as  $M_{\text{gas}} / (M_* + M_{\text{gas}})$ .

We generate the  $Z$ –SSFR relation and show it as a function of the gas mass fraction in Fig. 2 (right). Although with our  $H\text{I}$  sample it is only possible to see the low-mass branch in this relationship, it is clear that the gas mass fraction of galaxies increases as the SSFR increases, consistent with our proposed cartoon model. The black triangles in Fig. 2 (right) correspond to SDSS galaxies in the AL-

FALFA and GASS fields with no  $H\text{I}$  detection and  $M_* > 10^{11} M_\odot$ . A linear fit to these data is given by  $\log(\text{SSFR}) = -3.509 - 0.7184x$ , where  $x = 12 + \log(\text{O}/\text{H})$ .

Fig. 2 also suggests that there is a relation between the gas mass fraction and the SSFR. This indicates, regardless of the  $M_*$ , that the intrinsic rate at which a galaxy is forming stars depends strongly on the gas mass fraction. This relationship is shown in Fig. 3(a). Galaxies with a high gas mass fraction show a very steep relation with SSFR. On the other hand, galaxies with a low gas mass fraction have uniformly flat and low SSFRs in which the lack of gas would prevent galaxies from forming stars. Indeed, there is an inflection point between this abrupt change at  $\log(\text{SSFR}) \sim -9.9$ , in agreement with the dividing line seen in Fig. 1, that motivated the cartoon model of Fig. 2.

The relations between the gas mass fraction with the stellar mass and metallicity are shown in Figs 3(b) and (c). Similarly to Fig. 3(a), these relations show steep and flat tendencies for high and low gas mass fractions, respectively. Galaxies with high gas mass fractions have low metallicities and low masses. This suggests, as downsizing indicates, that low-mass galaxies assemble their stars on longer time-scales compared to massive galaxies. Galaxies with very low gas mass fractions have assembled their stellar mass, exhausted their gas and reached high stellar masses and high metallicities. As a result, galaxies with low gas mass fraction will show a flat relation against stellar mass and metallicity, as seen in Figs 3(b) and (c), respectively. To further refine this picture,  $H\text{I}$  measurements for massive galaxies are necessary.

Another way to see the influence of the gas fraction on metals is through the  $M_*$ – $Z$  relation shown in Fig. 4(a). Since low-mass

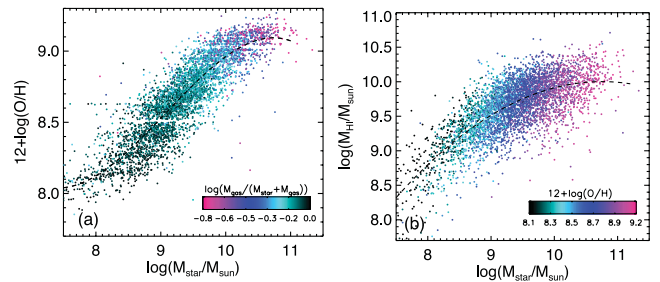


**Figure 4.** (a)  $M_*$ – $Z$  relation colour coded from low (magenta) to high (green)  $H\text{I}/M_*$  content. (b)  $\log(M_{H\text{I}}/M_\odot)$  versus  $\log(M_*/M_\odot)$  relation colour coded from low (green) to high (magenta) metallicity.

galaxies are actively forming stars they show a high H I gas fraction but low metallicity, while massive galaxies have finished forming stars, exhausting their H I and reaching high metallicities. A fit to this relation gives:  $12 + \log(\text{O}/\text{H}) = 47.751 - 13.903x + 1.5839x^2 - 0.05815x^3$ , with  $x = \log(M_*/M_\odot)$ .

Two important extensive variables analysed here are the stellar mass and the total H I in galaxies. The relationship between both is shown in Fig. 4(b). It is interesting to note that low-mass galaxies have a larger amount of mass in H I than in stars, which supports the scenario described in this section. Galaxies with a higher mass in stars were more efficient at forming stars in the past, resulting in the current amount of H I that is relatively smaller, although still larger in an absolute sense, than in low stellar mass systems. A fit to this relation gives:  $\log(M_{\text{HI}}/M_\odot) = -8.368 + 3.4166x - 0.1588x^2$ , with  $x = \log(M_*/M_\odot)$ .

## 5 DISCUSSION AND CONCLUSIONS

A key question to answer to have a general picture of this model is, why do low metallicity galaxies have either high SSFRs or low SSFRs but almost nothing in between? In the picture presented here, galaxies evolve in a downsizing fashion with two independent mechanisms that lead to having a galaxy with low metallicities: (i) A high-mass galaxy will be at low metallicity today if it exhausted its available fuel for SF and can no longer continue to enrich its ISM. (ii) A low-mass galaxy will be at low metallicity while it slowly forms stars, taking longer to enrich its ISM.

These different scenarios lead naturally to the dearth of mid-range SSFRs for the very low metallicity systems. Massive galaxies at low metallicity imply less and less SF the lower the metallicity needing to be maintained. Vice versa, for the low-mass galaxies, the metallicity stays low if the system is young and has a high amount of H I and SSFR.

As observed in Figs 1 and 2, within the range of stellar masses present at a given metallicity, the lower mass end will still have higher SSFRs than the higher mass end, but the difference compared to the lowest metallicities will be reduced. This is because the higher mass galaxies can have progressively more SF and still stay at mid-range to higher metallicities, while the lower mass galaxies could have had a more bursty SF in the past due to a higher amount of H I, which today would result in a high metallicity, low H I content and hence low SSFR.

We can argue that more SF increases the metallicity, which is sensible for massive galaxies, in which their SSFR increases as metallicity increases. It is noteworthy, however, that this does not apply for low-mass galaxies, which follow the opposite behaviour.

Therefore, we propose that galaxies will follow a downsizing scenario in which the H I content is an important driver of their evolution. Low-mass galaxies with a large amount of H I will process their gas on longer time-scales and thus show low metallicities today. On the other hand, low-mass galaxies with a lower H I might have evolved differently. These galaxies might have experienced a more bursty SF in the past that exhausted their gas and increased their metallicity.

Additionally, a combination of the infall of pristine gas and environment could play an important role here. In this second scenario, infall can be more significant for low-mass galaxies, diluting their

metallicity, and provide pristine fuel for high SSFRs. It is possible, even perhaps likely, that a combination of such scenarios are at play. To explain the observations presented here, and further explore the cartoon model proposed, more detailed simulations targeted at this problem are necessary.

## ACKNOWLEDGEMENTS

We thank the referee for suggestions that have improved the clarity of our analysis. GAMA is a joint European–Australasian project based around a spectroscopic campaign using the Anglo-Australian Telescope. GAMA is funded by the STFC (UK), the ARC (Australia), the AAO and the participating institutions. The GAMA website is <http://www.gama-survey.org/>. Funding for the SDSS and SDSS-II was provided by the Alfred P. Sloan Foundation. MALL thanks the ARC for funding through Super Science Fellowship FS110200023.

## REFERENCES

- Abazajian K. N. et al., 2009, *ApJS*, 182, 543  
 Baldwin J., Phillips M., Terlevich R., 1981, *PASP*, 93, 5  
 Brinchmann J., Charlot S., White S. D. M., Tremonti C., Kauffmann G., Heckman T., Brinkmann J., 2004, *MNRAS*, 351, 1151  
 Calura F., Pipino A., Chiappini C., Matteucci F., Maiolino R., 2009, *A&A*, 504, 373  
 Catinella B. et al., 2010, *MNRAS*, 403, 683  
 Driver S. P. et al., 2011, *MNRAS*, 413, 971  
 Erb D. K., 2008, *ApJ*, 674, 151  
 Finlator K., Davé R., 2008, *MNRAS*, 385, 2181  
 Gunawardhana M. L. P. et al., 2011, *MNRAS*, 415, 1647  
 Gunn J. E. et al., 2006, *AJ*, 131, 2332  
 Haynes M. P. M. et al., 2011, *AJ*, 142, 170  
 Hughes T. M., Cortese L., Boselli A., Gavazzi G., Davies J. I., 2013, *A&A*, 550, A115  
 Kauffmann G. et al., 2003a, *MNRAS*, 341, 33  
 Kauffmann G. et al., 2003b, *MNRAS*, 346, 1055  
 Lara-López M. A., Cepa J., Bongiovanni A., Castañeda H., Pérez García A. M., Fernández Lorenzo M., Póvic M., Sánchez-Portal M., 2009a, *A&A*, 493, L5  
 Lara-López M. A., Cepa J., Bongiovanni A., Pérez García A. M., Castañeda H., Fernández Lorenzo M., Póvic M., Sánchez-Portal M., 2009b, *A&A*, 505, 529  
 Lara-López M. A., Bongiovanni A., Cepa J., Pérez García A. M., Sánchez-Portal M., Castañeda H. O., Fernández Lorenzo M., Póvic M., 2010, *A&A*, 519, A31  
 Lara-López M. A., López-Sánchez Á. R., Hopkins A. M., 2013a, *ApJ*, 764, 178  
 Lara-López M. A. et al., 2013b, *MNRAS*, submitted  
 Lebouteiller V., Heap S., Hubeny I., Kunth D., 2013, *A&A*, 553, A16  
 López-Sánchez Á. R., 2010, *A&A*, 521, A63  
 Pettini M., Pagel B. E. J., 2004, *MNRAS*, 348, L59  
 Strauss M. A. et al., 2002, *AJ*, 124, 1810  
 Taylor E. N. et al., 2011, *MNRAS*, 418, 1587  
 Tremonti C. A. et al., 2004, *ApJ*, 613, 898  
 Yates R. M., Kauffmann G., Guo Q., 2012, *MNRAS*, 422, 215  
 Zhang W., Li C., Kauffmann G., Zou H., Catinella B., Shen S., Guo Q., Chang R., 2009, *MNRAS*, 397, 1243

This paper has been typeset from a  $\text{\TeX}/\text{\LaTeX}$  file prepared by the author.